JOURNAL OF CATALYSIS 87, 398–413 (1984)

An XPS Study of Metal–Support Interactions on Pd/SiO_2 and Pd/La_2O_3

THEO H. FLEISCH,* ROBERT F. HICKS,† AND ALEXIS T. BELL†

*Amoco Research Center, Standard Oil Company (Indiana), Naperville, Illinois 60566, †Materials and Molecular Research Division, Lawrence Berkeley Laboratory and Department of Chemical Engineering, University of California, Berkeley, California 94720

Received August 23, 1983; revised December 1, 1983

The electronic properties of palladium supported on SiO_2 and La_2O_3 were investigated by X-ray photoelectron spectroscopy. Spectra were collected after each stage of catalyst preparation: deposition of the palladium chloride precursor, oxidation in air at 623 K, and reduction in H_2 at 573 K. The Pd $3d_{5/2}$ binding energies recorded following precursor deposition and oxidation were the same on both catalysts. However, after reduction the Pd $3d_{5/2}$ binding energies of the Pd/La_2O_3 samples shifted below the corresponding values for metallic Pd, while the Pd $3d_{5/2}$ binding energies of the Pd/SiO_2 samples did not. Furthermore, the binding energies for the Pd/La_2O_3 samples decreased with increasing metal loading, the largest Pd particles apparently exhibiting the greatest interaction. A maximum shift of −0.7 eV relative to the Pd foil value was observed for 8.8% Pd/La_2O_3. This binding energy shift is interpreted as arising from a change in the chemical state of Pd, i.e., that Pd supported on La_2O_3 is more electronegative than zero-valent Pd alone. A model is proposed which suggests that a thin covering of the La_2O_3 support lies on a portion of the Pd surface. This covering is partially reduced during H_2 treatment at 573 K and, because of the electropositive nature of La, the additional charge is distributed amongst the surface Pd atoms. It should be noted that the La_2O_3 support surface after H_2 reduction is a complex mixture of $La(OH)_3$, LaO(OH), La_2O_3, and $La_2(CO_3)_3$. The exact composition of the support depended strongly on the reduction temperature and the amount of Pd deposited.

INTRODUCTION

Supported Pd has been found to be an active catalyst for the synthesis of CH_3OH from CO and H_2 (*1*). Several recent studies (*2–9*) have shown that the specific activity and selectivities of Pd for this reaction are strongly affected by the composition of the support. Particularly high methanol turnover frequencies have been obtained using supports such as La_2O_3 and Nd_2O_3. Pd supported on these metal oxides produces CH_3OH almost exclusively, with only a small coproduction (<2%) of CH_4. The lowest turnover frequencies and selectivity for CH_3OH synthesis are observed for Pd supported on ZrO_2 and TiO_2. It has also been reported that the manner of support preparation, and possibly the presence of impurities, can affect the catalytic properties of Pd supported on a material of supposedly fixed composition. Thus, for example, the specific activity of silica-supported Pd can vary by 20-fold and the selectivity for CH_3OH can vary between 0 and 100% depending on the type of silica used.

These remarkable effects of support composition on the catalytic properties of Pd strongly suggest that the support can alter the electronic properties of Pd, and by this means the manner in which Pd surface atoms interact with CO and H_2. A technique which should be able to provide evidence for a change in the electronic properties of Pd due to metal–support interactions is X-ray photoelectron spectroscopy (XPS). The utility of XPS for this purpose has been recently demonstrated (10–14) in studies devoted to understanding the Strong Metal–Support Interactions (SMSI) which occur between Group VIII metals and TiO_2. XPS studies of supported Pd

0021-9517/84 $3.00

have also been conducted. Bozan-Verduraz *et al.* (*15*) have shown that XPS can be used to identify the composition of the palladium chloride complex obtained upon impregnating SiO_2, Al_2O_3, and TiO_2 with palladium chloride solution. More recently, Lee *et al.* (*16*) have found that the addition of ZrO_2 to Pd/α-Al_2O_3 catalysts resulted in reduction of the Pd $3d_{5/2}$ binding energy relative to that observed in metallic Pd, suggesting that the Pd had become negatively charged.

In this paper, we report a systematic XPS investigation of the chemical properties of Pd/SiO_2 and Pd/La_2O_3. The discussion begins with an examination of catalyst preparation. In particular, XPS is used to identify the composition of the palladium chloride compounds deposited on the support surfaces, and then follow their decomposition during subsequent oxidation and reduction. The remainder of the paper focuses on the nature of the metal–support interaction. The presumption underlying this part of the investigation was that the interaction may exhibit characteristics indicative of a chemical reaction. If so, the support, as well as the metal, should be affected by the metal–support interaction. Changes in support composition and electronic properties were identified by collecting spectra of the supports in the presence and absence of Pd. A second consequence of this hypothesis is that the extent of the interaction should depend on the relative amount of metal in contact with the support. This possibility was studied by varying the Pd weight loading from 0.25 to 9.0%, and determining its effect on the chemical properties of the catalyst surface. The relevance of the results reported here to the chemisorption of CO and the catalytic properties of Pd/SiO_2 and Pd/La_2O_3 will be presented separately.

EXPERIMENTAL

Sample Preparation

The Pd precursor, assumed to be H_2PdCl_4, was prepared following the method of Aben (*17*). This material was produced by dissolving $PdCl_2$ in concentrated HCl and then evaporating the solution to dryness. The Pd/SiO_2 samples were prepared by incipient wetness impregnation of Cab-O-Sil HS-5 silica (BET surface area, 300 m^2/g) with a solution of H_2PdCl_4 dissolved in 1 *N* HCl. The additional HCl was required to maintain the Pd complex in solution. Most of the Pd/La_2O_3 samples were prepared by ion exchange. The La_2O_3 was donated by Union Molycorp. Prior to ion exchange, the support was refluxed in boiling water, during which time the La_2O_3 underwent complete hydrolysis to $La(OH)_3$ (BET surface area ~11 m^2/g) (*18*). The H_2PdCl_4 was dissolved in water without further addition of HCl, and added dropwise to the $La(OH)_3$ slurry at 298 K. Following addition of the Pd precursor, the slurry was heated to 338 K and held for 12 h. It should be noted that the solution changed from a yellow to a light-coffee color when it was heated to 338 K. After the holding period, the slurry was filtered and the filtrate was washed with several liters of distilled water. The Pd/SiO_2 and Pd/La_2O_3 samples, so obtained, were dried in a vacuum oven at 338 K. The samples were then calcined in a 21% O_2/He mixture at 623 K for 2 h and reduced in pure H_2 at 573 K for 3 h. After reduction, the samples were stored in a desiccator until use in the XPS experiments. One Pd/La_2O_3 sample, containing 0.2 wt% Pd, was prepared by the adsorption and decomposition of $Pd(\pi$-$C_3H_5)_2$. This method of sample preparation is described by Ryndin *et al.* (*3*).

Table 1 lists the weight loading of Pd, the concentration of exposed Pd atoms, C_{Pd_s}, and the dispersion of Pd for all of the samples used in this study. The Pd weight loading of the reduced samples was determined by X-ray fluorescence and quantitative analysis. The concentration of exposed Pd atoms was determined by H_2–O_2 titration at 298 K, using the pulsed flow technique (*3, 19–21*). The dispersion was calculated by dividing C_{Pd_s} by the total metal concentration.

TABLE 1

Dispersion and Concentration of Exposed Pd Atoms

Catalyst	D_{Pd} (%)	C_{Pd_s} (mmol/g Cat)
0.75% Pd/SiO_2	28	0.020
2.00% Pd/SiO_2	35	0.065
5.10% Pd/SiO_2	26	0.126
9.00% Pd/SiO_2	18	0.153
0.20% Pd/La_2O_3[a]	21	0.004
0.25% Pd/La_2O_3	30	0.007
0.70% Pd/La_2O_3	18	0.012
1.90% Pd/La_2O_3	16	0.029
1.95% Pd/La_2O_3	11	0.021
5.00% Pd/La_2O_3	9	0.041
8.80% Pd/La_2O_3	8	0.069

[a] Derived from $Pd(\pi\text{-}C_3H_5)_2$; all others by ion exchange of H_2PdCl_4.

XPS Apparatus and Procedure

The XPS experiments were performed in a Hewlett–Packard 5950B ESCA spectrometer using monochromatic Al$K\alpha$ radiation ($h\nu$ = 1486.6 eV). The base pressure of the instrument was 1×10^{-9} Torr. A Hewlett–Packard electron flood gun was used to minimize surface charging effects. The electron-binding energy scale was calibrated by assigning 284.6 eV to the C 1*s* peak position, as suggested by Wagner (*22*). In the case of the silica-supported samples, somewhat better experimental reproducibility was achieved by referencing the electron-binding energy axis to Si 2*p* at 103.2 eV. The binding energies reported here are accurate to ±0.2 eV, unless noted otherwise. XPS surface compositions were calculated from photoelectron peak areas after correcting for instrumental parameters, photoionization cross sections (*23*), and differences in electron escape depth (*24*). The C 1*s*, O 1*s*, and La $3d_{5/2}$ spectra were deconvoluted using an algorithm obtained from Surface Science Laboratories (Palo Alto, Calif.).

A quartz tube reactor was mounted onto the XPS vacuum system so that samples could be pretreated and transferred into the spectrometer without exposure to air. Reduction was carried out in 1 atm of pure H_2 at temperatures between 573 and 773 K, using a flow rate of 80 (STP) cm^3/min.

RESULTS AND DISCUSSION

Pd/SiO_2

XPS spectra of the 2% Pd/SiO_2 sample were taken after each stage of sample preparation: drying of the chloride precursor, calcination, and reduction. The peaks observed for the Pd $3d_{5/2}$ and $3d_{3/2}$ levels are given in Fig. 1. It is apparent that the positions of these peaks shift to lower binding energies proceeding from the supported precursor to the reduced catalyst. Since the extent of the binding energy shift is the same for the two 3*d* levels, the interpretation of these observations will be restricted to the $3d_{5/2}$ level.

The Pd $3d_{5/2}$ spectrum of the dried catalyst is composed of two overlapping peaks at 337.9 and 337.0 eV and a weak shoulder at 335.9 eV. The positions of these peaks are similar to those observed by Bozon-Verduraz *et al.* (*15*) following the impregnation of SiO_2, TiO_2, and Al_2O_3 with $PdCl_2$ dissolved in a 2 *N* HCl solution. Bands occurring at 338.1, 337.8, 337.1, and 336.1 eV were assigned by the authors to $PdCl_4^{2-}$, $PdCl_2$, $PdCl_2(H_2O)_2$, and $Pd(H_2O)_4^{2+}$, respectively. The assignments of the first two peaks are consistent with the work of Kumar *et al.* (*25*), which indicates a binding energy of 338.0 ± 0.3 eV for K_2PdCl_4 and a binding energy of 337.5 ± 0.2 eV for $PdCl_2$.

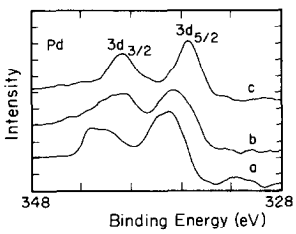

FIG. 1. Pd 3*d* spectra taken during the preparation of the 2.0% Pd/SiO_2 sample: (a) after impregnation with the Pd precursor and drying; (b) after calcining in air at 623 K; (c) after reduction in H_2 at 573 K.

In view of these results, it is proposed that the peaks at 337.9, 337.0, and 335.9 eV, seen in spectrum a (Fig. 1) can be assigned to $PdCl_4^{2-}$, $PdCl_2(H_2O)_2$, and $Pd(H_2O)_4^{2+}$, respectively. The presence of $PdCl_4^{2-}$ is expected, since a uv–visible spectrum of the impregnating solution exhibited bands at 221, 279, 331, and 445 nm which are characteristic of this species (*26*). The hydrated complexes are probably formed via a stepwise hydrolysis of $PdCl_4^{2-}$, as indicated below.

$$PdCl_4^{2-} + 2H_2O \rightleftarrows PdCl_2(H_2O)_2 + 2Cl^-$$

$$PdCl_2(H_2O)_2 + 2H_2O \rightleftarrows Pd(H_2O)_4^{2+} + 2Cl^-$$

Following calcination of the dried Pd/SiO_2 sample in air at 623 K, the Pd $3d_{5/2}$ binding energy shifts to 336.3 eV. This value agrees well with the peak maximum observed for PdO (*27, 28*). Examination of the Pd $3d_{5/2}$ portion of spectrum b in Fig. 1 suggests that it is composed of more than one peak. The higher energy component of this peak could be due to some residual chloride species not fully decomposed during calcination. Hydrogen reduction at 573 K shifts the binding energy of the Pd $3d_{5/2}$ peak to 335.3 eV. A small peak can also be seen at 337.0 eV which is attributable to some residual $PdCl_2(H_2O)_2$. This feature could be completely removed by carrying out a second reduction of the sample (cf. Fig. 2). The position of the peak at 335.3 eV is in very good agreement with that observed in other studies of silica-supported Pd (*15*) and with a binding energy reported for metallic Pd of 335.2 eV (*25, 28, 30*).

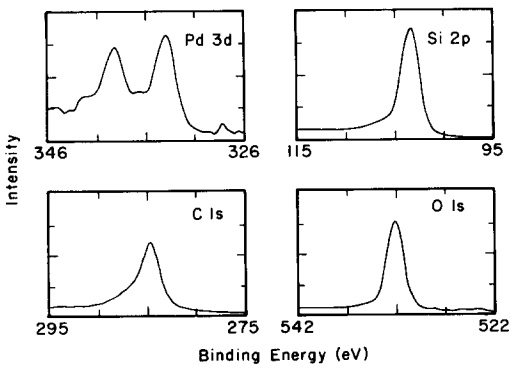

FIG. 2. XPS spectra of 2.0% Pd/SiO_2 following reduction in H_2 for 4 h at 573 K.

TABLE 2

Elemental Binding Energies for Pd/SiO_2 Samples

Catalyst	Binding energies (eV)[a]		
	Pd $3d_{5/2}$	Si $2p$	O $1s$
0.75% Pd/SiO_2	335.4	103.3	532.9
2.00% Pd/SiO_2	335.3	103.2	532.7
5.10% Pd/SiO_2	335.1	103.2	532.9
9.00% Pd/SiO_2	335.3	103.2	532.7

[a] Referenced to C $1s$ at 284.6 eV.

The spectra of the four silica-supported samples taken after reduction at 573 K were very similar. Figure 2 illustrates the peaks observed for photoemission from the Pd $3d$, Si $2p$, O $1s$, and C $1s$ levels. The binding energies of the peak maxima are given in Table 2. It is noted that the binding energy for each element is virtually independent of Pd loading.

Although Pd dispersions varied by almost twofold, no particle size-dependent shifts in the Pd $3d_{5/2}$ binding energy, of the kind observed by Takasu *et al.* (*29*) and Mason (*40*), were detected on the Pd/SiO_2 samples. The absence of this effect is a direct consequence of the low dispersion of Pd. For dispersions between 35 and 18%, the average metal crystallite size is estimated to be between 50 and 150 Å. Studies by Takasu *et al.* (*29*) indicate that Pd crystallites in this size range are expected to exhibit the electronic properties of bulk metal Pd.

The elemental surface composition of the four Pd/SiO_2 samples is given in Table 3. These data represent an average of the results obtained before reduction, after reduction at 573 K, and after reduction at 673 K. The data for the 2% Pd/SiO_2 catalyst show that repeated reduction does not alter

TABLE 3

Surface Composition for Pd/SiO_2 Samples

Catalyst	Surface composition (%)			
	Pd	Si	O	C
0.75% Pd/SiO_2	0.03	22.5	74.5	2.9
2.00% Pd/SiO_2	0.09	25.0	72.7	2.3
5.10% Pd/SiO_2	0.20	22.1	74.0	3.7
9.00% Pd/SiO_2	0.34	23.2	70.1	6.4
2.00% Pd/SiO_2				
Air exposed	0.09	25.0	72.5	2.5
H_2 reduced (573 K)[a]	0.08	25.1	72.8	2.0
H_2 reduced (673 K)[a]	0.09	24.9	72.8	2.5

[a] Reduction time—4 h.

the surface composition relative to that deduced from the air-exposed sample. It was also noted that the small amount of graphitic carbon present, characterized by a binding energy of 284.6 eV, was not affected by the hydrogen treatments.

The binding energies for the Si 2*p* and O 1*s* peaks, presented in Table 2, agree with those reported in the literature for SiO_2 (*30*). The data in Table 3 indicate that the O/Si ratio ranges between 3.3 and 2.9, with an average of 3.1. The high value of this ratio relative to the bulk stoichiometric ratio of 2.0 is consistent with the composition of a silica surface covered by hydroxyl groups.

The atomic percentage of Pd determined from the XPS spectra increases from 0.03 to 0.34% as the Pd weight loading increases from 0.75 to 9.00%. A low value of the atomic percentage is expected, since the support has a high BET surface area (300 m^2/g) and is sparsely covered by the Pd microcrystallites. The correlation of the atomic percentage of Pd with the concentration of exposed Pd atoms, C_{Pd_s}, is shown in Fig. 3. For small values of C_{Pd_s}, the percentage of Pd detected by photoemission rises nearly linearly. However, above C_{Pd_s} = 0.10 mmol/g, the curve deviates upward.

The trend in the data shown in Fig. 3 can be explained on the basis of a simplified model proposed by Angevine *et al.* (*31*). This model assumes that the catalyst consists of a uniform distribution of cubes of active component on a flat, semi-infinite support surface. If the fraction of the support covered by metal is small and the size of the cubes is large compared to the mean free path for inelastic scattering of an electron, then,

$$\frac{I_M}{I_S} = \frac{K_{MS} N_M}{d_p S_{BET}} \tag{1}$$

In Eq. (1) $I_{M,S}$ is the peak area of a particular XPS line in M, the active component, or S, the support; N_M is the number of atoms of element M per gram of catalyst; d_p is the length of a cube edge; S_{BET} is the BET surface area; and $K_{M,S}$ is a constant characteristic of the metal–support system examined. Since, in the present case, the support composition does not vary with metal content, and the metal covers a small percentage of the support,

$$\frac{I_M}{I_S} \simeq K_f f_M \tag{2}$$

where f_M is the atomic percentage of Pd determined by XPS and K_f is a proportionality constant. By combining Eqs. (1) and (2) we obtain

$$f_M = \frac{K_{M,S}}{K_f} \frac{N_M}{d_p S_{BET}} \tag{3}$$

Equation 3 can now be rewritten in terms of the concentration of exposed metal at-

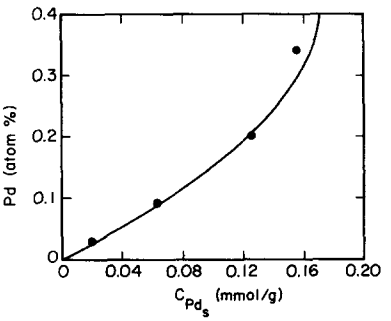

FIG. 3. Correlation of the atomic percentage of surface Pd, determined by XPS, with C_{Pd_s} for Pd/SiO_2.

oms, C_{M_s}, and the metal dispersion, D_M, by using the relations,

$$C_{M_s} = N_M D_M \quad (4)$$

$$D_M = K_s \frac{d_a}{d_p} \quad (5)$$

In Eq. (5), d_a is the diameter of the metal atom, and K_s is a proportionality factor which depends on the shape of the metal particles and the nature of the particle size distribution. Introducing Eqs. (4) and (5) into Eq. (3) gives

$$f_M = \frac{K_{M,S}}{K_f K_s} \frac{C_{M_s}}{d_a S_{BET}} \quad (6)$$

Equation (6) predicts that f_M should be a linear function of C_{M_s} provided K_s and S_{BET} are constant. This relationship is in good agreement with the data presented in Fig. 3 for $C_{M_s} = C_{Pd_s} \leq 0.10$ mmol/g. The upward deviation from the linear relation, seen for $C_{Pd_s} \geq 0.10$ mmol/g is most likely due to a decrease in the value of K_s caused by a change in the shape and/or particle size distribution of the supported Pd.

Pd/La_2O_3

Figure 4 presents a Pd 3*d* spectrum for the dried 1.9% Pd/La_2O_3 sample prior to calcination. Only a single peak is observed at 336.9 eV. The assignments proposed by Bozon-Verduraz *et al.* (*15*), which were discussed in the section on the silica-supported Pd, suggest that this peak can be ascribed to a palladium aquochloride species.

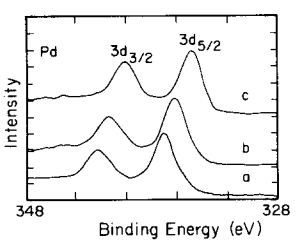

FIG. 4. Pd 3*d* spectra taken during the preparation of the 1.9% Pd/La_2O_3 sample: (a) after impregnation with the Pd precursor and drying; (b) after calcining in air at 623 K; (c) after reduction in H_2 at 573 K.

This interpretation is supported, in part, by the uv–visible spectrum of the H_2PdCl_4 solution used to introduce Pd onto the support. The bands observed at 208, 234, 303, and 416 nm are distinctly different from those characteristic of $PdCl_4^{2-}$ (280, 335, and 475 nm) and $PdCl_2$ (500 nm) (*15*). Jørgensen (*26*) indicates that the uv–visible spectrum of $PdCl_2(H_2O)_2$ is characterized by a band at 416 nm. While the position of this band coincides with one of the bands observed in the spectrum of the impregnating solution, a straightforward identification of the dissolved species cannot be made.

After calcination, the binding energy of the Pd $3d_{5/2}$ peak is shifted to 336.2 eV. The position of this peak is nearly identical to that observed for the calcined Pd/SiO_2 sample (see Fig. 1) and is in good agreement with that found for PdO (*27, 28*). Reduction of the sample at 573 K causes a shift in the Pd $3d_{5/2}$ peak to 334.7 eV. The position of this peak is 0.6 eV lower than that observed for the reduced Pd/SiO_2 sample and is 0.4 eV lower than that observed for a Pd foil. The noticeable deviation in the binding energy for lanthanum oxide-supported Pd, relative to that for metallic Pd, suggests that the support has an influence on the electronic properties of the metal. Further evidence for this, and a discussion concerning possible origins, is presented below.

Spectra for photoelectron emission from the Pd 3*d*, La 3*d*, O 1*s*, and C 1*s* levels of the 2% Pd/La_2O_3 sample, reduced at 573 K, are shown in Fig. 5. The Pd 3*d* peaks are identical to spectrum c in Fig. 4. The La 3*d* spectrum consists of two doublets. The satellites appearing on the high energy side of the $3d_{5/2}$ and $3d_{3/2}$ peaks are believed to result from competitive core-hole screening by nearly degenerate ligand 2*p* and empty La 4*f* orbitals (*32–35*). The La $3d_{3/2}$ and $3d_{5/2}$ core levels are observed at 850.8 and 834.0 ± 0.4 eV, respectively, and the corresponding satellite-split is 4.2 eV. The O 1*s* spectrum consists of two features: a strong peak at 531.0 eV and a shoulder at 528.5

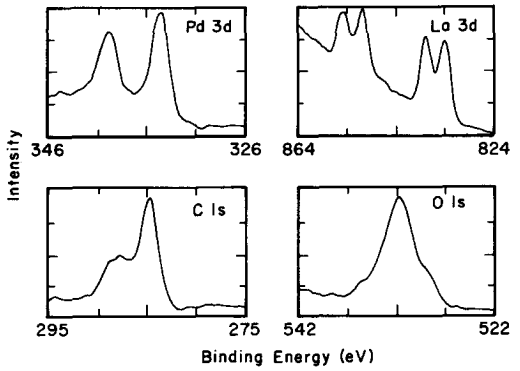

FIG. 5. XPS spectra of 1.9% Pd/La_2O_3 following reduction in H_2 for 4 h at 573 K.

eV. The first of these peaks is characteristic of OH^- and CO_3^{2-}, and the latter of O^{2-}. The C 1*s* spectrum is also made up of two peaks. The more intense peak at 284.6 is characteristic of graphitic carbon, whereas the less intense peak at 289.3 ± 0.4 eV is characteristic of CO_3^{2-} anions (*30*).

Effects of Heat Treatment on La_2O_3

In strong contrast to what was observed for silica-supported Pd, the photoelectron spectra of lanthanum oxide-supported Pd evidenced changes in the support composition during reduction. The effects of reduction temperature on the spectra of the support elements are presented in Fig. 6 and in Tables 4 and 5. As the extent of reduction increases, the positions of the La 3*d* peaks shift to lower binding energies, and the satellite-split increases. The O 1*s* portion of the air-exposed sample shows only a single

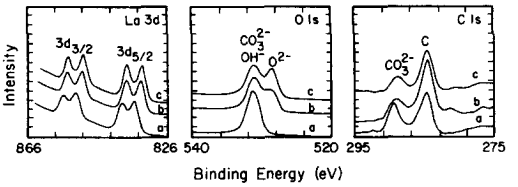

FIG. 6. Effects of H_2 reduction on the XPS spectra of the support for 0.7% Pd/La_2O_3: (a) exposed to air at 298 K; (b) reduced in H_2 for 4 h at 573 K; (c) reduced in H_2 for 4 h at 673 K following acquisition of spectrum b.

peak at 531.2 eV. As noted above, this feature is characteristic of OH^- and CO_3^{2-} anions. Following reduction, this peak decreases in intensity and a second peak appears at 528.6 eV which is characteristic of O^{2-} anions. These changes are accompanied by a reduction in the O/La ratio from 2.4 for the air exposed sample to 1.3 for the sample reduced at 673 K. The C 1*s* portion of the spectrum attributable to CO_3^{2-} anions decreases in intensity and shifts to lower binding energies with increasing reduction temperature. The graphitic carbon peak, on the other hand, remains unchanged throughout the sequence of H_2 treatments. The position and shape of the Pd $3d_{5/2}$ peak was also found to be unaffected by the reduction temperature.

Several experiments were carried out with the support alone to determine whether effects similar to those shown in Fig. 6 could be observed in the absence of Pd. The starting material for these experiments, referred to as activated La_2O_3, had undergone the same preparation steps as

TABLE 4

Influence of Reduction on the Elemental Binding Energies for the 0.7% Pd/La_2O_3 Sample

Treatment	Pd $3d_{5/2}$	La $3d_{5/2}$[a]	O 1*s*	C 1*s*[a]
None (air exposed)	336.2,334.9	834.6(3.5)[b]	531.2	289.9,284.6
H_2 reduced (573 K)[c]	334.8	833.8(4.2)	531.1,528.6	289.3,284.6
H_2 reduced (673 K)[c]	334.8	833.5(4.5)	531.3,528.7	288.9,284.6

[a] La $3d_{5/2}$ and CO_3^{2-} C 1*s* positions ∓ 0.4 eV, all others ∓ 0.2 eV.
[b] Satellite-split.
[c] Reduction time—4 h.

TABLE 5

Influence of Reduction on the Surface Composition of the 0.7% Pd/La_2O_3 Sample

Treatment	Surface composition (%)			
	Pd	La	O	C
None (air exposed)	0.5	23.0	55.4	17.7
H_2 reduced (573 K)[a]	0.6	35.7	50.9	12.8
H_2 reduced (673 K)[a]	0.6	36.2	46.1	17.2

[a] Reduction time—4 h.

TABLE 6

Effects of Heat Treatment on the Elemental Binding Energies for La_2O_3

Treatment	Binding energy (eV)[a]		
	La $3d_{5/2}$	O 1*s*	C 1*s*
Activated La_2O_3[b]	834.9 (3.3)[c]	530.9	287.6,284.6
H_2, 573 K, 3 h	834.9 (3.7)	530.9	288.3,284.6
H_2, 773 K, 3 h	834.4 (3.8)	530.6,528.4	288.3,284.6
N_2, 573 K, 2 h[d]	834.7 (3.7)	530.8	288.1,284.6
N_2, 773 K, 3 h	833.6 (4.2)	530.8,528.6	288.8,284.6
N_2, 873 K, 17 h	833.9 (4.0)	531.1,528.6	289.6,284.6
$La(OH)_3$[e]	835.9 (3.7)	532.1	284.6
La_2O_3[e]	834.7 (4.5)	530.1	284.6

[a] La $3d_{5/2}$ and CO_3^{2-} C 1*s* positions ±0.4 eV, all others ±0.2 eV.

[b] La_2O_3 converted to $La(OH)_3$ and then calcined at 623 K and heated in H_2 at 573 K.

[c] Satellite-split.

[d] Heating in N_2 was initiated with a fresh sample of activated La_2O_3.

[e] Data from Refs. (*36, 37*).

the catalysts: hydrolysis of La_2O_3 to $La(OH)_3$ followed by vacuum drying at 338 K, oxidation at 623 K, and reduction at 573 K. Tables 6 and 7 indicate the effects of heating the activated La_2O_3. It is seen that gas composition has little effect on the observed changes in binding energy and elemental composition. On the other hand, treating the sample at consecutively higher temperatures causes the support to change in a fashion qualitatively similar to that exhibited by 0.7% Pd/La_2O_3. As the temperature increases, the La $3d_{5/2}$ binding energy decreases, the satellite-split increases, the O/La ratio decreases, and at 773 K the O^{2-} peak appears in the spectrum. Comparison of the data in Tables 4 and 5 with those in Tables 6 and 7 shows that the extent to which these changes occur is much greater when Pd is present. In particular, after heating the 0.7% Pd/La_2O_3 sample 4 h at 673 K, 40% of the oxygen detected by XPS was O^{2-}; by contrast, after heating the activated La_2O_3 for 3 h at 773 K, only 14% of the oxygen detected was O^{2-}. These results, and others presented below, clearly indicate that Pd catalyzes changes in the support composition.

The effects of heat treating the support either in the presence or absence of Pd, can be attributed to a gradual dehydration of the support. Prior to heating, the XPS spectra of 0.7% Pd/La_2O_3 and activated La_2O_3 show no evidence for O^{2-} and an O/La ratio of nearly three. This suggests that the support is fully hydrated to $La(OH)_3$. This interpretation is consistent with the observations of Rosynek and Magnuson (*18*) who reported that La_2O_3 will rehydrate upon exposure to < 10 Torr of water vapor at 298 K. Upon heating in either H_2 or N_2, four changes occur in the spectrum of the support: the La $3d_{5/2}$ binding energy decreases, the La $3d_{5/2}$ satellite-split increases, the O^{2-} component of the O 1*s* spectrum increases, and the O/La ratio decreases. These trends reflect a

TABLE 7

Effects of Heat Treatment on the Surface Composition of La_2O_3

Treatment	Surface composition (%)		
	La	O	C
Activated La_2O_3[a]	19.5	56.8	23.8
H_2, 573 K, 3 h	26.8	54.1	19.2
H_2, 773 K, 3 h	27.2	51.3	21.5
N_2, 573 K, 2 h[b]	23.5	56.8	19.7
N_2, 773 K, 3 h	27.0	50.1	22.9
N_2, 873 K, 17 h	30.3	46.0	23.7

[a] La_2O_3 converted to $La(OH)_3$ and then calcined at 623 K and heated in H_2 at 573 K.

[b] Heating in N_2 was initiated with a fresh sample of activated La_2O_3.

gradual loss of water from the support and its progressive conversion from $La(OH)_3$ to La_2O_3. Brundle and co-workers (*36, 37*) have reported that the La $3d_{5/2}$ binding energy is 1.2 eV lower, and the satellite-split 1 eV greater, for La_2O_3 compared to $La(OH)_3$. A discrepancy of about 1 eV exists, though, between the La $3d_{5/2}$ and O 1*s* binding energies reported here and those reported by Brundle and co-workers. The source of this discrepancy cannot be established since these authors give no indication of the source of their samples, nor the methods used for sample preparation.

Rosynek and Magnuson (*18*) found that $La(OH)_3$ decomposes to La_2O_3 in two distinct stages upon heating under vacuum. At 473 K, $La(OH)_3$ is converted to LaO(OH). This compound then decomposes to La_2O_3 when the temperature is raised above 573 K. It is doubtful, though, that complete conversion of $La(OH)_3$ to La_2O_3 ever occurred during this study, since the portion of the O 1*s* spectrum associated with O^{2-} never rose above 40%, even after the support had been heated at 873 K for 17 h. Furthermore, Raman spectra (*38*) taken of the heat treated catalyst samples showed evidence for $La(OH)_3$ and La_2O_3, as well as additional bands believed to be due to LaO(OH). It must be concluded, therefore, that after heating, the support is a mixture of $La(OH)_3$, LaO(OH), and La_2O_3. A certain amount of carbonate must also be present, since the peak at 288.5 eV, associated with CO_3^{2-} is never eliminated from the C 1*s* spectrum. The presence of carbonate anions is expected in view of the known reactivity of lanthanum oxide and hydroxide with CO_2, and that lanthanum carbonate does not decompose at temperatures below 973 to 1073 K (*18*).

Negative Pd Binding Energy Shift

The palladium loading was found to influence both the Pd $3d_{5/2}$ binding energy and the composition of the support. The data for all seven of the Pd/La_2O_3 samples are given in Tables 8 and 9.

TABLE 8

Elemental Binding Energies for Pd/La_2O_3 Samples

Catalyst[a]	Binding energies (eV)[b]		
	Pd $3d_{5/2}$	La $3d_{5/2}$	O 1*s*
0.20% Pd/La_2O_3	334.9	834.3	531.5,529.0
0.25% Pd/La_2O_3	335.3	834.3	531.3,529.0
0.70% Pd/La_2O_3	334.8	833.8	531.1,528.6
1.90% Pd/La_2O_3	334.7	834.0	531.0,528.5
1.95% Pd/La_2O_3	334.5	833.9	531.8,529.1
5.00% Pd/La_2O_3	334.5	834.3	531.8,529.0
8.80% Pd/La_2O_3	334.4	834.4	531.1,528.7
Pd-Black/La_2O_3	335.0	—	—

[a] Reduced in H_2 for 4 h at 573 K.
[b] La $3d_{5/2}$ position ±0.4 eV, all others ±0.2 eV.

The binding energy for the Pd $3d_{5/2}$ peak is plotted in Fig. 7a as a function of Pd dispersion, D_{Pd}, and in Fig. 8 as a function of the concentration of exposed Pd atoms, C_{Pd_s}. It is apparent that the binding energy decreases progressively with either decreasing values of D_{Pd} or increasing values of C_{Pd_s}. At its lowest value, the binding energy lies 0.7 eV below that for metallic Pd. The binding energy data for the Pd/SiO_2 samples are also shown in Fig. 7a for comparison. While the range of metal dispersions on the two supports are comparable, the data points for the Pd/SiO_2 samples lie close to the binding energy for metallic Pd, and show no evidence of a change in binding energy with dispersion.

TABLE 9

Surface Composition of Pd/La_2O_3 Samples

Catalyst[a]	Surface composition (%)			
	Pd	La	O	C
0.20% Pd/La_2O_3	0.2	34.3	48.6	15.9
0.25% Pd/La_2O_3	0.2	30.0	50.0	19.8
0.70% Pd/La_2O_3	0.6	35.7	50.9	12.8
1.90% Pd/La_2O_3	1.3	24.4	55.5	18.8
1.95% Pd/La_2O_3	1.5	14.0	52.8	31.6
5.00% Pd/La_2O_3	2.3	25.9	49.4	22.4
8.80% Pd/La_2O_3	5.0	19.4	53.0	22.7

[a] Reduced in H_2 for 4 h at 573 K.

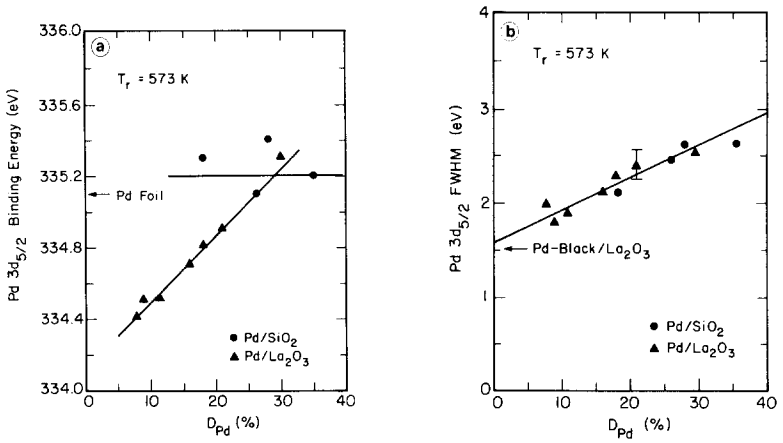

FIG. 7. (a) Correlation of the Pd $3d_{5/2}$ binding energy with D_{Pd} for Pd/SiO_2 and Pd/La_2O_3. (b) Correlation of the Pd $3d_{5/2}$ FWHM with D_{Pd} for Pd/SiO_2 and Pd/La_2O_3.

While not shown in Figs. 7a and 8, XPS results were also obtained for dilute mixtures of Pd-black and La_2O_3. For such mixtures, the Pd $3d_{5/2}$ binding energy, following H_2 reduction at 573 K, was 335.0 eV. This value is within the experimental accuracy of the binding energy measured for a Pd foil (335.1 eV). The close agreement in the measured value of the binding energies for large Pd particles dispersed in an insulating matrix and Pd foil indicates that accurate binding energy values can be obtained using the procedures described in this paper. It also implies that the graphitic carbon, used as a reference element, is in good electrical contact with the metal and very likely resides upon it as well as on the support. The validity of using the C 1*s* peak as a reference point is further substantiated by the observation that the Pd $3d_{5/2}$ binding energies for the palladium chloride precursor on La_2O_3 and the oxidized Pd on La_2O_3 are both in good agreement with the binding energies reported for $PdCl_2(H_2O)_2$ and PdO, respectively.

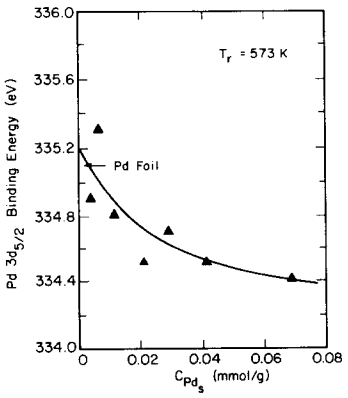

FIG. 8. Correlation of Pd $3d_{5/2}$ binding energy with C_{Pd_s} for Pd/La_2O_3.

The full width at half maximum (FWHM) of the Pd $3d_{5/2}$ peak for the Pd/La_2O_3 samples is plotted versus Pd dispersion in Fig. 7b. Once again, for comparison, the data for the Pd/SiO_2 samples are included. Both sets of data lie along a single straight line and show that the FWHM increases with increasing dispersion. The FWHM was also measured for the mixture of Pd-black and La_2O_3, and was found to be 1.5 eV. This is consistent with the value obtained by extrapolating the straight line passing through the data to D_{Pd} = 0–3% and it is in good agreement with what is expected for metals supported on an insulator. Using an Au foil as a standard, the instrument is tuned so that the Au $4f_{7/2}$ FWHM is 0.8 eV. Insulating supports typically add more than 0.5 eV to the FWHM of all lines even with the use of an electron flood gun. Consequently, a FWHM of greater than 1.3 eV is anticipated for a low metal dispersion on an insulating support.

The data given in Table 8, and Figs. 7a and 8, demonstrate very clearly that the binding energy of the Pd $3d_{5/2}$ state for Pd supported on La_2O_3 can lie below that of metallic Pd by as much as 0.7 eV. Shifts of a similar nature have been observed by several authors in recent XPS studies of supported Group VIII metals. In the work of Lee *et al.* (*16*), it was found that the binding energy for the Pd $3d_{5/2}$ state decreased from 335.2 to 334.8 eV upon the addition of ZrO_2 to Pd supported on α-Al_2O_3. Negative shifts of the order of 0.2 to 1.6 eV have been reported for Rh/TiO_2 (*12, 13*), Ni/TiO_2, Pt/TiO_2, and $Pt/SrTiO_3$ (*10, 11, 14*) following reduction of these catalysts at temperatures in excess of 773 K.

The interpretation of core level binding energy shifts for supported metals is difficult, since the observed deviations from the binding energy of the pure metal can reflect changes in both the initial and final states of the metal (*39*). These effects are influenced not only by the chemical state of the metal, but also by the size of the supported metal crystallites. When small metal particles are placed on a support, a positive binding energy shift relative to the bulk value is often observed. In the limit of an isolated metal atom on a support, positive shifts can be as great as 1.6 eV (*40*). Several authors (*10, 11, 14, 39, 46*) have suggested that these effects are due to differences in final-state, extraatomic relaxation. It is thought that in small metal clusters there are not enough metal atoms in the particle to completely screen core-holes created by photoemission, and that it is the incomplete screening which gives rise to a positive shift. On the other hand, Mason (*40*) has recently presented evidence that the shift in binding energy with particle size is due to a rehybridization of the (*s,p*)-*d* orbitals and depends only on the average coordination number of the atoms in the particle. In this regard, Mason shows that the photoemission spectra of clusters and alloys are identical provided both the substrate and the host metal weakly interact with the cluster orbitals. All authors agree that the effects of particle size are negligible, if the supported metal particles are large enough to exhibit bulk-like valence structure.

Takasu *et al.* (*29*) studied the changes in the electronic structure of Pd supported on SiO_2 as a function of metal particle size. It was found that when the Pd particles reached a size sufficient for the UPS spectrum to be indistinguishable from that observed for Pd foil, a positive shift in the Pd $3d_{5/2}$ binding energy relative to the foil value was no longer observed. The dispersion of the Pd/La_2O_3 samples studied here ranges between 10 and 30%, decreasing with increasing metal loading (see Table 1). The estimated average diameter of the Pd microcrystallites is, therefore, between 60 and 180 Å. Based on the criteria established by Takasu *et al.* (*29*), these particles well exceed the minimum size required to exhibit bulk-like valence structure. As a consequence, the shift in the Pd $3d_{5/2}$ binding energy as a function of D_{Pd} must be ascribed to a change in the chemical state of the metal. This interpretation is consistent with the results obtained for silica-supported Pd. The Pd particles on silica are about the same size as those on lanthanum oxide, and yet, the Pd $3d_{5/2}$ binding energies for Pd/SiO_2 are independent of D_{Pd} (see Fig. 7a). The direction of the binding energy shift for the Pd/La_2O_3 samples and the absence of any anomalies in the shape of the Pd peaks suggests that the lanthanum oxide-supported Pd is more electronegative than the Pd foil.

Model of Metal–Support Interaction

In a theoretical study, Horsley (*41*) examined the interaction of a Pt atom with a TiO_x cluster. This system was chosen to represent Pt supported on TiO_2. It was concluded that if Ti is reduced from the 4+ to the 3+ state, approximately 0.6 electrons will transfer from the Ti cation to the Pt atom. Recently, it has been shown that there is a reproducible −0.2 eV shift in the Rh $3d_{5/2}$ binding energy for Rh/TiO_2 reduced

above 673 K (*12, 13*). Since high-temperature reduction of TiO_2-supported transition metals may lead to a substantial increase in metal dispersion (*47, 48*), the chemical shift could be offset by a positive particle size-dependent shift, as discussed above. In this case, the chemical shift may be greater than −0.5 eV, a value in agreement with Horsley's theoretical prediction.

We propose that during sample activation the La_2O_3 support is reduced, and that this is responsible for the negative binding energy shift. While it is recognized that the reducibility of $La(OH)_3$ or La_2O_3 is substantially less than that of TiO_2, there is reason to believe that the surfaces of refractory oxides may be reducible. For example, Weller and Montagna (*42, 43*) have suggested that at 723 to 823 K, the surface of pure Al_2O_3 undergoes reduction. Evidence for a similar reaction has also been presented by Kunimori *et al.* (*44*) in a study of metal–support interactions in Pt/Al_2O_3.

The partial reduction of $La(OH)_3$, LaO(OH), and La_2O_3 might be represented as

$$1.\ La(OH)_3 + x\mathrm{Pd} + \frac{1}{2}H_2 \rightleftarrows LaPd_xO + 2H_2O$$

$$2.\ LaO(OH) + x\mathrm{Pd} + \frac{1}{2}H_2 \rightleftarrows LaPd_xO + H_2O$$

$$3.\ La_2O_3 + 2x\mathrm{Pd} + H_2 \rightleftarrows 2LaPd_xO + H_2O$$

Hydrogen is assumed to adsorb on the surface of the Pd microcrystallites and to diffuse to the interface between the microcrystallite and the support material. The final products of reactions 1 through 3 should not be regarded as stoichiometric compounds, but rather as representations of the adducts formed between x atoms of Pd present at the metal–support interface and the surface of the partially reduced support. Because of the strongly electropositive nature of La, it is expected that the Pd atoms will become more electronegative.

The possibility that the shifts in Pd $3d_{5/2}$ binding energy for the Pd/La_2O_3 samples are due to La–Pd intermetallic compounds can be excluded. The formation of such substances would require the complete reduction of portions of the support—an unlikely occurrence. Moreover, recent XPS studies by Hillebrecht *et al.* (*45*) have shown that the Pd $3d_{5/2}$ binding energies for La–Pd intermetallic compounds all lie above that for metallic Pd and show an increasing upscale shift with increasing La/Pd ratio.

While reactions 1 through 3 provide a means for rationalizing the observation of a negative shift in the Pd binding energy, it remains to be explained why such an effect should be observed for the very large Pd crystallites (60 to 180 Å) present on the lanthanum oxide surface. If the only point of contact between the metal crystallites and the support is at the bottom of the crystallites, then one would expect the electrons of the Pd atoms in the crystallite bulk to screen out the charge transferred to the Pd atoms present at the metal–support interface. Under such circumstances, the Pd binding energy would not be expected to shift. The fact that the binding energy does shift suggests the picture shown in Fig. 9. Here, the surface of the Pd microcrystallite is assumed to be partly covered by small patches of support material which migrate onto the Pd during sample pretreatment. Upon reduction, these patches are expected to undergo reduction consistent with reactions 1 through 3. Since the adduct, $LaPd_xO$, is now present at the surface of the metal crystallites, the bulk Pd atoms

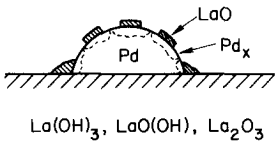

FIG. 9. Schematic illustration of the interaction of Pd with the support.

would no longer be as effective in screening out the effects of the metal–support interaction. The increase in absolute magnitude of the Pd binding energy shift with increasing metal loading, seen in Fig. 8, might then be attributed to an increase in the fraction of the metal crystallites covered by support material. It should be noted that the CO chemisorption characteristics of the Pd/La_2O_3 sample are consistent with the proposed model (*49*). The chemisorption experiments indicate that the exposed Pd atoms are segregated into two types of surfaces. One surface adsorbs a monolayer of CO. While the other surface does not adsorb CO, as if it is covered by a physical obstruction. Furthermore, the portion of the Pd surface blocked to CO chemisorption increases with increasing Pd weight loading.

The increased electronegativity of the surface Pd atom appears to be distributed uniformly over the Pd surface. As shown in Fig. 7b, the FWHM of the Pd $3d_{5/2}$ line is identical for Pd/La_2O_3 and Pd/SiO_2 samples of equivalent dispersion. Since only one chemical state of Pd assuredly exists on Pd/SiO_2, the same must be concluded for Pd/La_2O_3. This conclusion is further supported by CO chemisorption studies at 298 K (*49*), which evidence a considerable weakening of the CO bond strength on the exposed Pd atoms that do chemisorb CO. In addition, the FWHM correlation indicates that H_2–O_2 titration correctly measures the amount of exposed Pd atoms, including those postulated to be underneath the patches of LaO. For this to be true, the H_2 and O_2 must titrate the $LaOPd_x$ compound with the same stoichiometry as that for the uncovered Pd surface. This requirement is easily rationalized for $x = 1$:

$$\text{Uncovered:}\quad \text{Pd–H} + \frac{3}{4}\,O_2 \rightarrow \text{Pd–O} + \frac{1}{2}\,H_2O \quad (1)$$

$$\text{Covered:}\quad \text{LaOPd} + \frac{3}{4}\,O_2 \rightarrow La_2O_3 + \text{PdO} \quad (2)$$

The support covering is also expected to be thin so that the X rays can detect the Pd which is underneath the oxide layer. A thin LaO layer seems likely based on the observation that oxidizing the Pd/La_2O_3 at 298 K causes the formation of new sites for CO adsorption (*49*). These new sites are on the Pd surfaces which do not chemisorb CO in the reduced state, and they bond CO in an unusual way. The vibrational frequency of the infrared band for this form of chemisorbed CO is suggestive of a CO molecule which is bridge-bonded between a Pd atom and a support atom.

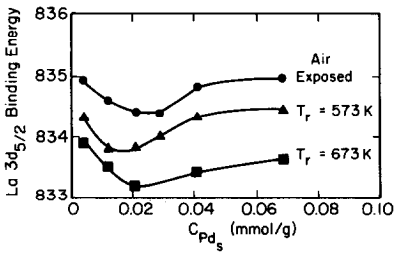

FIG. 10. Effects of H_2 reduction and C_{Pd_s} on the La $3d_{5/2}$ binding energy for Pd/La_2O_3.

Effects of Metal Loading on Surface Composition

The loading of Pd was also found to influence the La $3d$ binding energy, the surface concentration of La, the O/La ratio, and the distribution of peaks in the O $1s$ spectrum. These trends can be seen by inspection of Tables 8 and 9, and Figs. 10 through 12. Figure 10 shows that the binding energy for the La $3d_{5/2}$ peak passes through a minimum as the concentration of exposed Pd atoms increases. It is also noted that, consistent with the results presented earlier, the binding energy shifts to lower values as the temperature used to reduce the catalyst is increased. The influence of C_{Pd_s} on the near-surface concentrations of La^{3+} and O^{2-} is given in Fig. 11, whereas Fig. 12 illustrates the variation of the O/La ratio

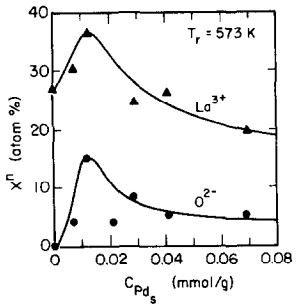

FIG. 11. Correlation of the atom percentages of La^{3+} and O^{2-} with C_{Pd_s} for Pd/La_2O_3.

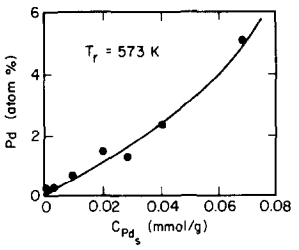

FIG. 13. Correlation of the atomic percentage of Pd, determined by XPS, with C_{Pd_s} for Pd/La_2O_3.

with C_{Pd_s}. With increasing Pd loading, and hence C_{Pd_s}, the percentages of La^{3+} and O^{2-} pass through a maximum, while the O/La ratio passes through a minimum. All of the extrema occur near C_{Pd_s} = 0.015 mmol/g. The patterns exhibited in Figs. 10 through 12 can be attributed to changes in the extent of conversion of $La(OH)_3$ to LaO(OH) and La_2O_3. It would appear that as the loading of Pd increases, the extent of dehydration at first increases, but then reaches a maximum and subsequently decreases. The cause for the maximum is unclear. One possibility is that the support dehydration is retarded by the water released in reactions 1 through 3 at higher metal loadings.

Figure 13 illustrates the variation of the atomic percentage of Pd, determined from XPS, with the concentration of exposed Pd atoms, C_{Pd_s}. As was found for Pd/SiO_2 in Fig. 3, the correlation is linear at first and then deviates upwards at higher values of C_{Pd_s}. The explanation for this trend is identical to that given in the discussion of Fig. 3. The atomic percentage of Pd on La_2O_3 is significantly higher than that for Pd/SiO_2, because the BET surface area of La_2O_3 is much lower than that of SiO_2.

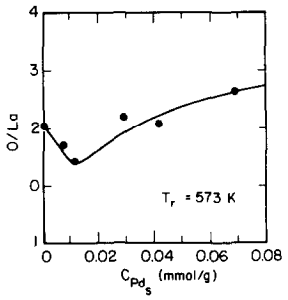

FIG. 12. Correlation of the O/La ratio with C_{Pd_s} for Pd/La_2O_3.

CONCLUSIONS

XPS spectra of silica-supported Pd show no evidence for metal–support interactions. The binding energy of electrons emitted from the Pd $3d_{5/2}$ level is only slightly greater than that for metallic Pd, and it is not affected by the weight loading of Pd on the support. By contrast, XPS spectra of lanthanum oxide-supported Pd provide clear indications of an interaction between Pd and the support. The Pd $3d_{5/2}$ binding energy lies below that of metallic Pd, the extent of the deviation increasing with increasing metal loading. The maximum deviation observed is surprisingly large: −0.7 eV for a metal loading of 8.8 wt%.

XPS spectra also reveal that the composition of the support changes during catalyst preparation. Prior to ion exchange with the Pd precursor, La_2O_3 is hydrated to increase its surface area. This causes a conversion of La_2O_3 to $La(OH)_3$. During calcination and reduction of the catalyst, the support is progressively dehydrated so that it finally consists of a mixture of $La(OH)_3$, LaO(OH), and La_2O_3. The extent of dehydration is accelerated by the presence of Pd, and it, too, is found to depend upon the metal loading. Below 0.7 wt% Pd, the degree of dehydration increases with loading.

Above 0.7 wt% Pd, though, this trend is reversed.

It is proposed that during catalyst preparation, a small part of the support material is deposited on the Pd particles, and that upon reduction in H_2 these deposits undergo partial reduction to form structures such as $LaPd_xO$. The palladium in these structures is more electronegative than the zero-valent metal. This interpretation would explain the observation of Pd $3d_{5/2}$ binding energies which are lower than that for metallic Pd.

ACKNOWLEDGMENTS

This work was supported by Standard Oil Company (Indiana) and by the Division of Chemical Sciences, Office of Basic Energy Sciences, U.S. Department of Energy under Contract DE-AC03-76SF00098.

REFERENCES

1. Poutsma, M. L., Elek, L. F., Ibarbia, P. A., Risch, A. P., and Rabo, J. A., *J. Catal.* **52,** 157 (1978).
2. Ichikawa, M., *Shokubai* **21,** 253 (1979).
3. Ryndin, Yu. A., Hicks, R. F., Bell, A. T., and Yermakov, Yu. I., *J. Catal.* **70,** 287 (1981).
4. Poels, E. K., von Broekhoven, E. H., von Barneveld, W. A. A., and Ponec, V., *React. Kinet. Catal. Lett.* **18,** 223 (1981).
5. Fajula, F., Anthony, R. G., and Lunsford, J. H., *J. Catal.* **73,** 237 (1982).
6. Kikuzono, Y., Kagami, S., Naito, S., Onishi, T., and Tamaru, K., *Faraday Discuss. Chem. Soc.* **72,** 135 (1982).
7. Ponec, V., *in* "Metal-Support and Metal-Additive Effects in Catalysis" (B. Imelik *et al.*, Eds.), p. 63. Elsevier, Amsterdam, 1982.
8. Poels, E. K., Koolstra, R., Geus, J. W., and Ponec, V., "Metal-Support and Metal-Additive Effects in Catalysis", (B. Imelik *et al.*, Eds.). Elsevier, Amsterdam, 1982.
9. Driessen, J. M., Poels, E. K., Hindermann, J. P., and Ponec, V., *J. Catal.* **82,** 26 (1983).
10. Bahl, M. K., Tsai, S. C., and Chung, Y. W., *Phys. Rev. B* **21,** 1344 (1980).
11. Kao, C. C., Tsai, S. C., Bahl, M. K., Chung, Y. W., and Lo, W. J., *Surf. Sci.* **95,** 1 (1980).
12. Sexton, B. A., Hughes, A. E., and Foger, K., *J. Catal.* **77,** 85 (1982).
13. Chien, S.-H., Shelimov, B. N., Resasco, D. E., Lee, E. H., and Haller, G. L., *J. Catal.* **77,** 301 (1982).
14. Fung, S. C., *J. Catal.* **76,** 225 (1982).
15. Bozon-Verduraz, F., Omar, A., Escard, J., and Pontvianne, B., *J. Catal.* **53,** 126 (1978).
16. Lee, Y., Inoue, Y., and Yasumori, I., *Bull. Chem. Soc. Jpn.* **54,** 3711 (1981).
17. Aben, P. C., *J. Catal.* **10,** 224 (1968).
18. Rosynek, M. P., and Magnuson, D. T., *J. Catal.* **46,** 402 (1977).
19. Benson, J. E., Hwang, H. S., and Boudart, M., *J. Catal.* **30,** 146 (1973).
20. Freel, J., *J. Catal.* **25,** 139 (1972).
21. Gruber, H. L., *Anal. Chem.* **34,** 1828 (1962).
22. Wagner, C. D., Zatko, D. A., and Raymond, R. H., *Anal. Chem.* **52,** 1445 (1980).
23. Scofield, J. H., *J. Electron Spectrosc. Relat. Phenom.* **8,** 129 (1976).
24. Ott, G. L., Fleisch, T. H., and Delgass, W. N., *J. Catal.* **60,** 394 (1979).
25. Kumar, G., Blackburn, J. R., Albridge, R. G., Moddeman, W. E., and Jones, M. M., *Inorg. Chem.* **11,** 296 (1972).
26. Jøorgensen, C. K., "Absorption Spectra and Chemical Bonding in Complexes." Pergamon, London, 1962.
27. Fleisch, T. H., and Mains, G. J., unpublished results.
28. Kim, K. S., Grossmann, A., and Winograd, N., *Anal. Chem.* **46,** 197 (1974).
29. Takasu, Y., Unwin, R., Tesche, B., and Bradshaw, A. M., *Surf. Sci.* **77,** 219 (1978).
30. Wagner, C. D., Riggs, W. M., Davis, L. E., and Moulder, J. F., *in* "Handbook of X-Ray Photoelectron Spectroscopy" (G. E. Muilenberg, Ed.). Perkin–Elmer, 1978.
31. Angevine, P. J., Vartuli, J. C., and Delgass, W. N., "Proceedings, 6th International Congress on Catalysis" (G. C. Bond, P. B. Wells, and F. C. Tompkins, Eds.). The Chemical Society, London, 1976.
32. Signorelli, A. J., and Hayes, R. G., *Phys. Rev. B* **8,** 81 (1973).
33. Crecelius, G., Wertheim, G. K., and Buchanan, D. N. E., *Phys. Rev. B* **18,** 6519 (1978).
34. Jørgensen, C. K., *in* "Structure and Bonding" (J. D. Dunitz, P. Hemmerich, R. H. Holm, J. A. Ibers, C. K. Jørgensen, J. B. Neilands, D. Reinen, and R. J. P. Williams, Eds.), Vol. 24. Springer–Verlag, New York, 1975.
35. Wendin, G., *in* "Structure and Bonding" (M. J. Clarke, J. B. Goodenough, P. Hemmerich, J. A. Ibers, C. K. Jørgensen, J. B. Neilands, D. Renin, R. Weiss, and R. J. P. Williams, Eds.), Vol. 45. Springer–Verlag, New York, 1981.
36. Siegmann, H. C., Schlapbach, L., and Brundle, C. R., *Phys. Rev. Lett.* **40,** 972 (1978).
37. Schlapbach, L., Seiler, A., Siegmann, H. C., Waldkirch, T. V., Zürcher, P., and Brundle, C. R., *Int. J. Hydrogen Energy* **4,** 21 (1979).
38. Chan, S., and Bell, A. T., unpublished results.
39. Delgass, W. N., Haller, G. L., Kellerman, R., and Lunsford, J. H., "Spectroscopy in Heterogeneous Catalysis." Academic Press, New York, 1979.

40. Mason, M. G., *Phys. Rev. B* **27,** 748 (1983).
41. Horsley, J. A., *J. Amer. Chem. Soc.* **101,** 2870 (1979).
42. Weller, S. W., and Montagna, A. A., *J. Catal.* **20,** 394 (1970).
43. Weller, S. W., and Montagna, A. A., *J. Catal.* **21,** 303 (1971).
44. Kunimori, K., Ikeda, Y., Soma, M., and Uchijima, T., *J. Catal.* **79,** 185 (1983).
45. Hillebrecht, F. U., Fuggle, J. C., Bennett, P. A., Zolnierek, Z., and Freiburg, Ch., *Phys. Rev. B* **27,** 2179 (1983).
46. Kim, K. S., and Winograd, N., *Chem. Phys. Lett.* **30,** 91 (1975).
47. Baker, R. T. K., Prestridge, E. B., and Garten, R. L., *J. Catal.* **59,** 293 (1979).
48. Tauster, S. J., Fung, S. C., Baker, R. T. K., and Horsley, J. A., *Science* **211,** 1121 (1981).
49. Hicks, R. F., Yen, Q.-J., and Bell, A. T., unpublished results.